NASA TECHNICAL MEMORANDUM

NASA TM X-1207

NASA TM X-1207

TRANSONIC AERODYNAMIC DAMPING AND OSCILLATORY STABILITY IN YAW AND PITCH FOR A MODEL OF A VARIABLE-SWEEP SUPERSONIC TRANSPORT AIRPLANE

by Bruce R. Wright and Benjamin T. Averett

Langley Research Center

Langley Station, Hampton, Va.

NATIONAL AERONAUTICS AND SPACE ADMINISTRATION • WASHINGTON, D. C. • MARCH 1966

NASA TM X-1207

TRANSONIC AERODYNAMIC DAMPING AND OSCILLATORY STABILITY IN YAW AND PITCH FOR A MODEL OF A VARIABLE-SWEEP SUPERSONIC TRANSPORT AIRPLANE

By Bruce R. Wright and Benjamin T. Averett

Langley Research Center
Langley Station, Hampton, Va.

NATIONAL AERONAUTICS AND SPACE ADMINISTRATION

For sale by the Clearinghouse for Federal Scientific and Technical Information
Springfield, Virginia 22151 – Price $0.30

TRANSONIC AERODYNAMIC DAMPING AND OSCILLATORY STABILITY IN YAW AND PITCH FOR A MODEL OF A VARIABLE-SWEEP SUPERSONIC TRANSPORT AIRPLANE

By Bruce R. Wright and Benjamin T. Averett
Langley Research Center

SUMMARY

19520

Wind-tunnel measurements were made in the Langley 8-foot transonic pressure tunnel to determine the aerodynamic damping and oscillatory stability in yaw and pitch for a model of a variable-sweep supersonic transport airplane (designated SCAT 15). All tests were made at an oscillation amplitude of 1° with the use of a forced-oscillation technique for angles of attack from -2° to 16°. The yaw tests were made at Mach numbers from 0.40 to 1.20 with corresponding Reynolds numbers, based on the mean aerodynamic chord of the fully swept wing, from 3.1×10^{6} to 5.8×10^{6}. The pitch tests were made only at a Mach number of 0.80 at a Reynolds number of 5.0×10^{6}.

For the model with the wing panels swept 25°, the yaw damping was positive and generally was linear with angle of attack at subsonic Mach numbers for the lower angles of attack. Both the damping and stability in yaw increased with increase in vertical-tail size. Above an angle of attack of about 12°, however, addition of vertical tails decreased the damping and resulted in negative damping at a Mach number of 0.80.

For a wing-sweep angle of 75° at the lower angles of attack, the damping and stability in yaw were positive and increased with vertical-tail size. Above about 6°, the yaw damping and stability parameters were very erratic and showed no systematic variations. Positive damping in pitch and positive values of the oscillatory-longitudinal-stability parameter were exhibited for all angles of attack at a Mach number of 0.80 for a wing-sweep angle of 25°.

Removal of the engine nacelles produced appreciable effects on the yaw parameters at the higher angles of attack. Only slight effects on the yaw damping and stability parameters were determined for tests with engine inlets plugged at Mach numbers of 0.95 and 1.20 for a wing-sweep angle of 75°.

autho

INTRODUCTION

A commercially successful supersonic transport airplane must have suitable performance, stability, and control characteristics in the design cruise condition and all other flight conditions. Therefore, in order to provide research information for the development of a successful supersonic commercial transport airplane, the National Aeronautics and Space Administration has undertaken a program to determine experimentally the aerodynamic characteristics of a number of proposed configurations.

Presented herein are the transonic aerodynamic damping and oscillatory-stability characteristics in pitch and yaw of one of the supersonic commercial air transport configurations designated SCAT 15. This configuration had a variable wing geometry in order to meet the requirements of both high- and low-speed flight. Both fixed and variable-sweep wing panels were employed. The fixed wing panel had a sweepback angle of 75° at the leading edge. The leading edge of the variable-sweep portion of the wing was swept back at an angle of 25° for low-speed flight, and this portion merged with the fixed portion to form an arrow wing for supersonic flight. The vertical and horizontal tails were mounted on the tips of the fixed wings as shown in figure 1.

The static-stability characteristics for the SCAT 15 configuration are presented in reference 1. The dynamic-stability tests presented herein were made in the Langley 8-foot transonic pressure tunnel at an oscillation amplitude of 1° with the use of a forced-oscillation technique for angles of attack from -2° to 16° with the model at zero sideslip. The Mach number for the yaw tests was varied from 0.40 to 1.20 with corresponding Reynolds numbers, based on the mean aerodynamic chord of the fully swept wing, from 3.1×10^{6} to 5.8×10^{6}. The reduced-frequency parameter was varied from 0.0152 to 0.0626 for the yaw tests. Pitch tests were made only at a Mach number of 0.80 at a Reynolds number of 5.0×10^{6} because of instrumentation difficulties. The reduced-frequency parameter was varied from 0.0145 to 0.0237 for the pitch tests.

Yaw tests were made with two sizes of vertical tails as well as with the vertical tails removed. Provisions could not be made to obtain the proper mass-flow rate for the engine inlets. Consequently, tests were made with the cylindrical engine inlets open, with the inlets plugged, and with the engine nacelles removed in order to provide a qualitative indication of the effect of engine inlets on the yawing dynamic-stability parameters.

SYMBOLS

The aerodynamic parameters are referred to the body system of axes originating at the oscillation center of the model as shown in figure 1. The International System of Units (SI) is used herein with U.S. Customary Units given parenthetically. (See ref. 2 for relationships between these systems.) The reference dimensions are based on the geometric characteristics of the model with the wings fully swept (excluding the horizontal tails) regardless of the actual test wing-sweep position.

b — model wing span of fully swept wing, 0.406 meter (1.333 ft)

C_Y, C_Z — damping coefficient about Y-axis and Z-axis of body, respectively, $\frac{\text{meter-newton-second}}{\text{radian}} \left(\frac{\text{ft-lb-sec}}{\text{rad}}\right)$

$\bar{c}$ — mean aerodynamic chord of fully swept wing, 0.397 meter (1.303 ft) (see fig. 1)

f — frequency of oscillation, cycles per second

I_Y, I_Z — moment-of-inertia coefficient about Y-axis and Z-axis of body, respectively, $\frac{\text{meter-newton-second}^2}{\text{radian}} \left(\frac{\text{ft-lb-sec}^2}{\text{rad}}\right)$

K_Y, K_Z — torsional-spring coefficient about Y-axis and Z-axis of body, respectively, $\frac{\text{meter-newton}}{\text{radian}} \left(\frac{\text{ft-lb}}{\text{rad}}\right)$

k — reduced-frequency parameter, $\frac{\omega \bar{c}}{2V}$ in pitch and $\frac{\omega b}{2V}$ in yaw, radians

M — free-stream Mach number

q — pitching velocity, radians/second

q_∞ — free-stream dynamic pressure, newtons/meter^2 (lb/ft^2)

R — Reynolds number based on $\bar{c}$

r — yawing velocity, radians/second

S — wing planform area of fully swept wing, 0.170 meter^2 (1.828 ft^2)

T_Y, T_Z — maximum torque required to oscillate model in pitch and in yaw, respectively, newton-meter (lb-ft)

V — free-stream velocity, meters/second (ft/sec)

α — angle of attack, degrees or radians; mean angle of attack, degrees

β — angle of sideslip, degrees or radians

η — phase angle between T_Y and Θ, degrees

Θ maximum angular displacement in pitch of model with respect to sting, radians

Λ leading-edge sweep angle of wing panel, degrees

λ phase angle between T_Z and $\bar{\psi}$, degrees

$\bar{\psi}$ maximum angular displacement in yaw of model with respect to sting, radians

ω angular velocity, $2\pi f$, radians/second

C_m pitching-moment coefficient, $\dfrac{\text{Pitching moment}}{q_\infty S\bar{c}}$

C_n yawing-moment coefficient, $\dfrac{\text{Yawing moment}}{q_\infty Sb}$

$C_{m_q} = \dfrac{\partial C_m}{\partial\left(\dfrac{q\bar{c}}{2V}\right)}$, per radian

$C_{m_\alpha} = \dfrac{\partial C_m}{\partial \alpha}$, per radian

$C_{m_{\dot{q}}} = \dfrac{\partial C_m}{\partial\left(\dfrac{\dot{q}\bar{c}^2}{4V^2}\right)}$, per radian

$C_{m_{\dot{\alpha}}} = \dfrac{\partial C_m}{\partial\left(\dfrac{\dot{\alpha}\bar{c}}{2V}\right)}$, per radian

$C_{n_r} = \dfrac{\partial C_n}{\partial\left(\dfrac{rb}{2V}\right)}$, per radian

$C_{n_\beta} = \dfrac{\partial C_n}{\partial \beta}$, per radian

$C_{n_{\dot{r}}} = \dfrac{\partial C_n}{\partial\left(\dfrac{\dot{r}b^2}{4V^2}\right)}$, per radian

$C_{n_{\dot{\beta}}} = \dfrac{\partial C_n}{\partial\left(\dfrac{\dot{\beta}b}{2V}\right)}$, per radian

$C_{m_q} + C_{m_{\dot{\alpha}}}$ damping-in-pitch parameter, per radian

$C_{m_\alpha} - k^2 C_{m_{\dot{q}}}$ oscillatory-longitudinal-stability parameter, per radian

$C_{n_r} - C_{n_{\dot{\beta}}} \cos \alpha$ damping-in-yaw parameter, per radian

$C_{n_\beta} \cos \alpha + k^2 C_{n_{\dot{r}}}$ oscillatory-directional-stability parameter, per radian

A dot over a quantity denotes the first derivative with respect to time. The expression $\cos \alpha$ appears in the directional parameters because these parameters are expressed in terms of the body system of axes.

DESCRIPTION OF APPARATUS

Model

Design dimensions of the model of this investigation are shown in figure 1. Detailed characteristics of the model are contained in reference 1. The model was aerodynamically similar to the proposed SCAT 15 airplane except for aft-fuselage modifications necessary to accommodate the support sting and oscillation mechanism. The fixed wing had a leading-edge sweep angle of 75°. The variable-sweep portion of the wing had a leading-edge sweep angle of 25° for tests at low Mach numbers, and this portion merged with the fixed portion to form an arrow wing with a sweep angle of 75° for tests at the higher Mach numbers. The vertical and horizontal tails were mounted on the tips of the fixed wings. Provisions were made for testing the model with vertical tails of two different sizes as well as with the vertical tails removed. Although the nonoperating engine inlets on the model were normally open to allow airflow, some tests were made with the inlets plugged and with the engine nacelles removed.

The model was made of magnesium and the vertical tails were made of stainless steel. Even though the test model was considered rigid, possible elastic distortion may have occurred because of the relatively thin wing panels. Three-dimensional roughness consisting of No. 60 carborundum grains was applied to the model to assure the existence of a turbulent boundary layer. The size and location of the three-dimensional roughness were computed by the method of reference 3.

Oscillation-Balance Mechanism

The forward portion of the oscillation-balance mechanism is shown in the photograph presented on page 6. Since the amplitude of the oscillation is small the rotary motion of an electric motor is used to provide essentially sinusoidal motion of constant amplitude to the balance through the crank and Scotch-yoke mechanism. Although constant amplitudes of $1/2^\circ$, 1°, and 2° can be obtained by using different cranks, an amplitude of 1° was used for these tests. The oscillation center was located at the model station corresponding to the proposed center of mass of the configuration. (See fig. 1.)

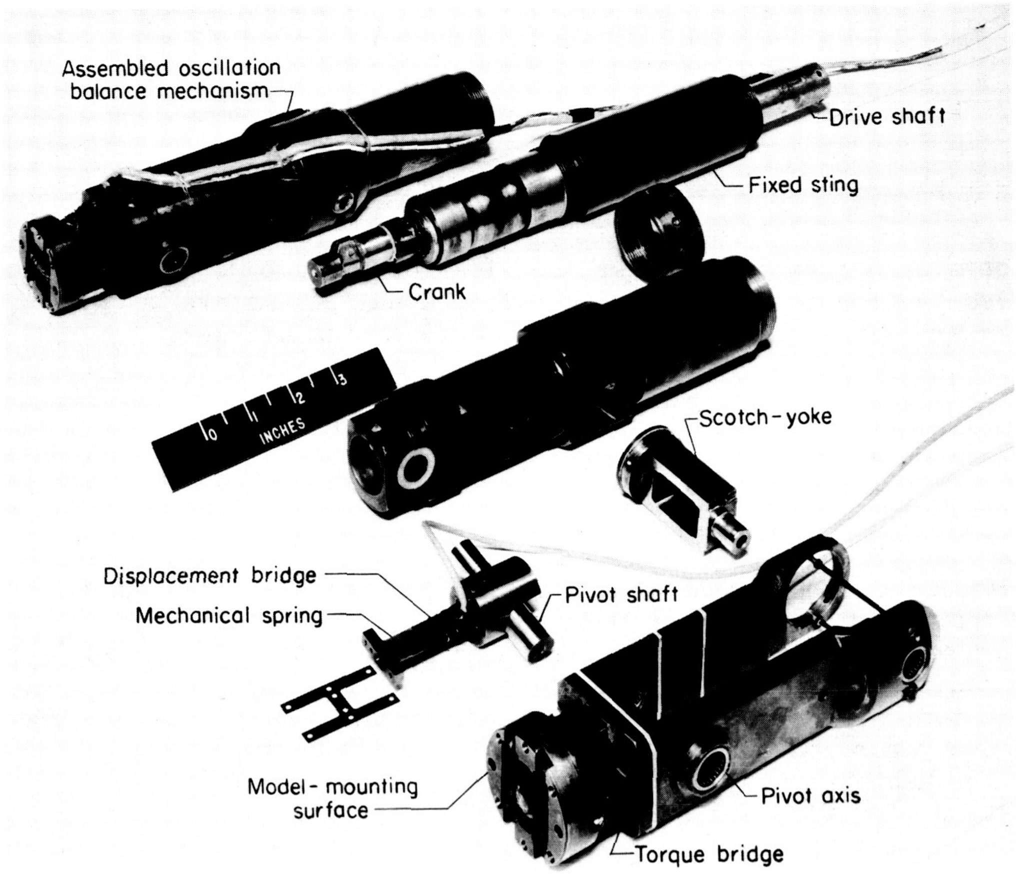

L-63-1969.1

As shown in the photograph, the strain-gage bridge which is used to measure the torque required to oscillate the model is located between the model-mounting surface and the pivot axis. The torque-bridge location eliminates the effects of pivot-bearing friction. Although the torque bridge is located forward of the pivot axis, compensating circuits shift the electrical centers of the bridge to the pivot axis so that all torques are measured with respect to the pivot axis of the oscillation balance.

A mechanical spring, which is attached to the fixed sting, is mounted within the oscillation balance and is connected to the front end of the oscillation balance through an H-shaped flexure. The mechanical spring allows the model-balance system to be oscillated at the frequency of velocity resonance. Although, with the forced-oscillation balance, the model may be oscillated at frequencies from about 4 to 30 cps, as explained in reference 4, the most accurate measurement of the damping coefficient is obtained at velocity resonance. As shown in the photograph, a strain-gage bridge is attached to the mechanical spring to provide a signal which is proportional to the angular displacement of the model with respect to the sting.

Wind Tunnel

The tests were made in the Langley 8-foot transonic pressure tunnel. The test section of this single-return closed-circuit wind tunnel is about 2.2 meters square (about 7.1 feet square) with the upper and lower walls slotted to permit continuous operation throughout the transonic speed range. Test-section Mach numbers up to about 1.30 can be obtained by controlling the speed of the tunnel-fan drive motor. The Mach number distribution is uniform throughout the test section, with the maximum deviation from the average free-stream Mach number on the order of 0.01 at the higher Mach numbers.

The sting-support system is designed to keep the model near the center line of the tunnel through an angle-of-attack range from -2° to 16° when used in conjunction with the oscillation-balance mechanism of these tests.

TEST CONDITIONS

The tests were made at an oscillation amplitude of 1° with the use of the previously described forced-oscillation technique for angles of attack from -2° to 16° with the model at zero sideslip. The Mach numbers for the yaw tests were varied from 0.40 to 1.20 with corresponding Reynolds numbers, based on the mean aerodynamic chord of the fully swept wing, from 3.1×10^6 to 5.8×10^6. The reduced-frequency parameter $\frac{\omega b}{2V}$ varied from 0.0152 to 0.0626 for the yaw tests. Because of instrumentation difficulties, the pitch tests were made only at a Mach number of 0.80 at a Reynolds number of 5.0×10^6. The reduced-frequency parameter $\frac{\omega \bar{c}}{2V}$ for the pitch tests varied from 0.0145 to 0.0237. The data are presented in figures 2 to 5 for the various test conditions as indicated by the following table:

Wing-sweep angle, Λ, deg	Engine inlets	Vertical tails	Mach number, M	Reynolds number, R	Figure
Directional					
25	Open	Large	0.40	3.1×10^6	2(a)
25	Open	Small	.40	3.1	2(a)
25	Open	Removed	.40	3.1	2(a)
25	Open	Large	.80	5.0	2(b)
25	Open	Small	.80	5.0	2(b)
25	Open	Removed	.80	5.0	2(b)
75	Open	Large	.95	5.5	3(a)
75	Open	Small	.95	5.5	3(a)
75	Open	Removed	.95	5.5	3(a)
75	Open	Large	1.20	5.6	3(b)
75	Open	Small	1.20	5.6	3(b)
75	Open	Removed	1.20	5.6	3(b)
75	Open	Large	.95	5.5	4(a)
75	Plugged	Large	.95	5.5	4(a)
75	Nacelles removed	Large	.95	5.5	4(a)
75	Open	Large	1.20	5.6	4(b)
75	Plugged	Large	1.20	5.6	4(b)
75	Nacelles removed	Large	1.20	5.6	4(b)
Longitudinal					
25	Open	Large	0.80	5.0×10^6	5

MEASUREMENTS AND REDUCTION OF DATA

Strain-gage bridges are used to measure the torque required to oscillate the model and the angular displacement of the model with respect to the sting. The signals are amplified and passed through mechanically coupled but electrically independent sine-cosine resolvers which rotate with constant angular velocity at the frequency of model oscillation. Each signal is resolved by the sine-cosine resolver into two components which are read on damped digital voltmeters. Details of the electronics used are given in reference 4.

From the computed values of the maximum torque required to oscillate the model in yaw T_Z, the maximum angular displacement in yaw of the model with respect to the sting Ψ, the phase angle λ between T_Z and Ψ, and the angular velocity of the forced oscillation ω (as explained in ref. 4), the damping coefficient for this single-degree-of-freedom system was computed as

$$C_Z = \frac{T_Z \sin \lambda}{\omega \Psi} \qquad (1)$$

Also, the spring-inertia parameter was computed as

$$K_Z - I_Z \omega^2 = \frac{T_Z \cos \lambda}{\Psi} \qquad (2)$$

where K_Z is the torsional-spring coefficient of the system and I_Z is the moment-of-inertia coefficient of the system about the Z-axis of the body.

For these tests, the damping-in-yaw parameter was computed as

$$C_{n_r} - C_{n_{\dot{\beta}}} \cos \alpha = -\frac{2V}{q_\infty S b^2}\left[\left(\frac{T_Z \sin \lambda}{\omega \Psi}\right)_{\text{wind on}} - \left(\frac{T_Z \sin \lambda}{\omega \Psi}\right)_{\text{wind off}}\right] \qquad (3)$$

and the oscillatory-directional-stability parameter was computed as

$$C_{n_\beta} \cos \alpha + k^2 C_{n_{\dot{r}}} = \frac{1}{q_\infty S b}\left[\left(\frac{T_Z \cos \lambda}{\Psi}\right)_{\text{wind on}} - \left(\frac{T_Z \cos \lambda}{\Psi}\right)_{\text{wind off}}\right] \qquad (4)$$

The value of $\left(\frac{T_Z \sin \lambda}{\omega \Psi}\right)_{\text{wind off}}$ is independent of oscillation frequency and is determined at the frequency of the wind-off velocity resonance, because, as explained in reference 4, maximum accuracy is obtained at the frequency of velocity resonance. The value of $\left(\frac{T_Z \cos \lambda}{\Psi}\right)_{\text{wind off}}$ is a function of the oscillation frequency and, therefore, is determined for each test value of the wind-on frequency.

From the computed values of the maximum torque required to oscillate the model in pitch T_Y, the maximum angular displacement in pitch of the model with respect to the sting Θ, the phase angle η between T_Y and Θ, and the angular velocity of the forced oscillation ω, the system characteristics in pitch were computed as

$$C_Y = \frac{T_Y \sin \eta}{\omega\Theta} \tag{5}$$

and

$$K_Y - I_Y\omega^2 = \frac{T_Y \cos \eta}{\Theta} \tag{6}$$

For these tests, the damping-in-pitch parameter was computed as

$$C_{m_q} + C_{m_{\dot{\alpha}}} = -\frac{2V}{q_\infty S\bar{c}^2}\left[\left(\frac{T_Y \sin \eta}{\omega\Theta}\right)_{\text{wind on}} - \left(\frac{T_Y \sin \eta}{\omega\Theta}\right)_{\text{wind off}}\right] \tag{7}$$

and the oscillatory-longitudinal-stability parameter was computed as

$$C_{m_\alpha} - k^2 C_{m_{\dot{q}}} = -\frac{1}{q_\infty S\bar{c}}\left[\left(\frac{T_Y \cos \eta}{\Theta}\right)_{\text{wind on}} - \left(\frac{T_Y \cos \eta}{\Theta}\right)_{\text{wind off}}\right] \tag{8}$$

As for the yaw tests, the value of $\left(\frac{T_Y \sin \eta}{\omega\Theta}\right)_{\text{wind off}}$ was determined at the frequency of the wind-off velocity resonance, and the wind-off and wind-on values of $\frac{T_Y \cos \eta}{\Theta}$ were determined at the same frequency of oscillation.

RESULTS AND DISCUSSION

Directional Results

The effects of vertical tails on the dynamic-stability characteristics in yaw for the model with the wing panels swept 25° are presented in figure 2 for Mach numbers of 0.40 and 0.80. At angles of attack below about 6°, the damping in yaw was positive (negative values of $C_{n_r} - C_{n_{\dot{\beta}}} \cos \alpha$) and generally linear with angle of attack for both Mach numbers; the oscillatory-directional stability was positive $\left(\text{positive values of } C_{n_\beta} \cos \alpha + k^2 C_{n_{\dot{r}}}\right)$ for all configurations but the one with the vertical tails removed. Both the damping and stability in yaw increased with the addition of vertical tails, with a greater increase for the larger vertical tail. Above an angle of attack of about 12°, however, addition of the vertical tails produced an adverse effect of decreased damping for both Mach numbers, and at a Mach number of 0.80 negative damping resulted for the configurations with large and small vertical tails. Although the flow phenomenon producing this negative damping is not understood at present, negative damping may be associated with wing-separation effects on the vertical tails.

The effects of the vertical tails on the dynamic-stability characteristics in yaw for the model with the wing panels swept 75° at Mach numbers of 0.95 and 1.20 are presented in figure 3. At angles of attack up to about 6°, the yaw damping and stability were positive and increased with an increase in the vertical-tail size. Above about 6°, the variations of the yaw damping and stability parameters with angle of attack were very erratic and indicated the probable presence of large areas of flow separation. The region of negative damping that was present at the high angles of attack for the model with the wing panels swept 25° at Mach numbers of 0.40 and 0.80 did not exist for the model with the panels swept 75° at Mach numbers of 0.95 and 1.20.

As mentioned previously, the proper mass-flow rate through the simulated engine inlets could not be obtained for this model. In order to provide a qualitative indication of the effect of the engine-inlet configuration on the directional dynamic-stability characteristics at Mach numbers of 0.95 and 1.20, investigations were made with the inlets open, with the inlets plugged, and with engine nacelles removed for the model with the wings swept 75°. As shown in figure 4, removal of the engine nacelles produced appreciable effects at the higher angles of attack. Although these effects were erratic and showed no systematic variation, they indicated the importance of simulating the engine nacelles on aircraft configurations of this type. Simulation of the exact amount of airflow, however, was less important than expected, as indicated by the fact that plugging the inlets had only a slight effect on the detailed damping or stability or the trends at Mach numbers of 0.95 and 1.20.

Longitudinal Results

Because of instrumentation difficulties longitudinal data were obtained only for $M = 0.80$ for the configuration with a wing-panel sweep of 25°, large vertical tails, and engine inlets open in these tests. Positive damping in pitch $\left(\text{negative values of } C_{m_q} + C_{m_{\dot{\alpha}}}\right)$ and near zero or positive (stable) values of the oscillatory-longitudinal-stability parameter were exhibited for all angles of attack at the oscillation-center location used (fig. 5).

CONCLUDING REMARKS

Wind-tunnel measurements were made in the Langley 8-foot transonic pressure tunnel to determine the aerodynamic damping and oscillatory stability in yaw and pitch for a model of a proposed variable-sweep supersonic transport airplane designated the SCAT 15.

For the model with the wing panels swept 25°, the yaw damping was positive and generally remained linear with angle of attack for angles below about 6°. At Mach numbers of 0.40 and 0.80 both the damping and stability increased with an increase in the vertical-tail size. Above an angle of attack of about 12°, however, addition of the vertical tails produced the adverse effect of decreased or negative damping for the subsonic test Mach numbers.

The model with the wing panels swept 75° was tested in yaw at Mach numbers of 0.95 and 1.20. At angles of attack up to about 6°, the damping and stability were positive and increased with an increase in the vertical-tail size. Above about 6°, the variations of the yaw damping and stability parameters were very erratic and inconsistent.

Pitch tests were made for the model with a wing-panel sweep of 25°, large vertical tails, and engine inlets open for a Mach number of 0.80. Positive damping in pitch and positive or near zero values of the oscillatory-longitudinal-stability parameter were exhibited for all test angles of attack.

Removal of the engine nacelles produced appreciable effects at the higher angles of attack for the configuration tested in yaw with the wings swept 75°. These effects indicate the importance of simulating the engine nacelles for dynamic-stability tests of aircraft configurations of this type. Tests with the engine inlets plugged indicated only a slight effect on the yaw damping or stability at Mach numbers of 0.95 and 1.20.

Langley Research Center,
National Aeronautics and Space Administration,
Langley Station, Hampton, Va., November 1, 1965.

REFERENCES

1. Henderson, William P.: Low-Speed Aerodynamic Characteristics of a Supersonic Transport Model With a Blended Wing-Body, Variable-Sweep Auxiliary Wing Panels, and Outboard Tail Surfaces. NASA TM X-993, 1964.

2. Mechtly, E. A.: The International System of Units – Physical Constants and Conversion Factors. NASA SP-7012, 1964.

3. Braslow, Albert L.; and Knox, Eugene C.: Simplified Method for Determination of Critical Height of Distributed Roughness Particles for Boundary-Layer Transition at Mach Numbers From 0 to 5. NACA TN 4363, 1958.

4. Braslow, Albert L.; Wiley, Harleth G.; and Lee, Cullen Q.: A Rigidly Forced Oscillation System for Measuring Dynamic-Stability Parameters in Transonic and Supersonic Wind Tunnels. NASA TN D-1231, 1962. (Supersedes NACA RM L58A28.)

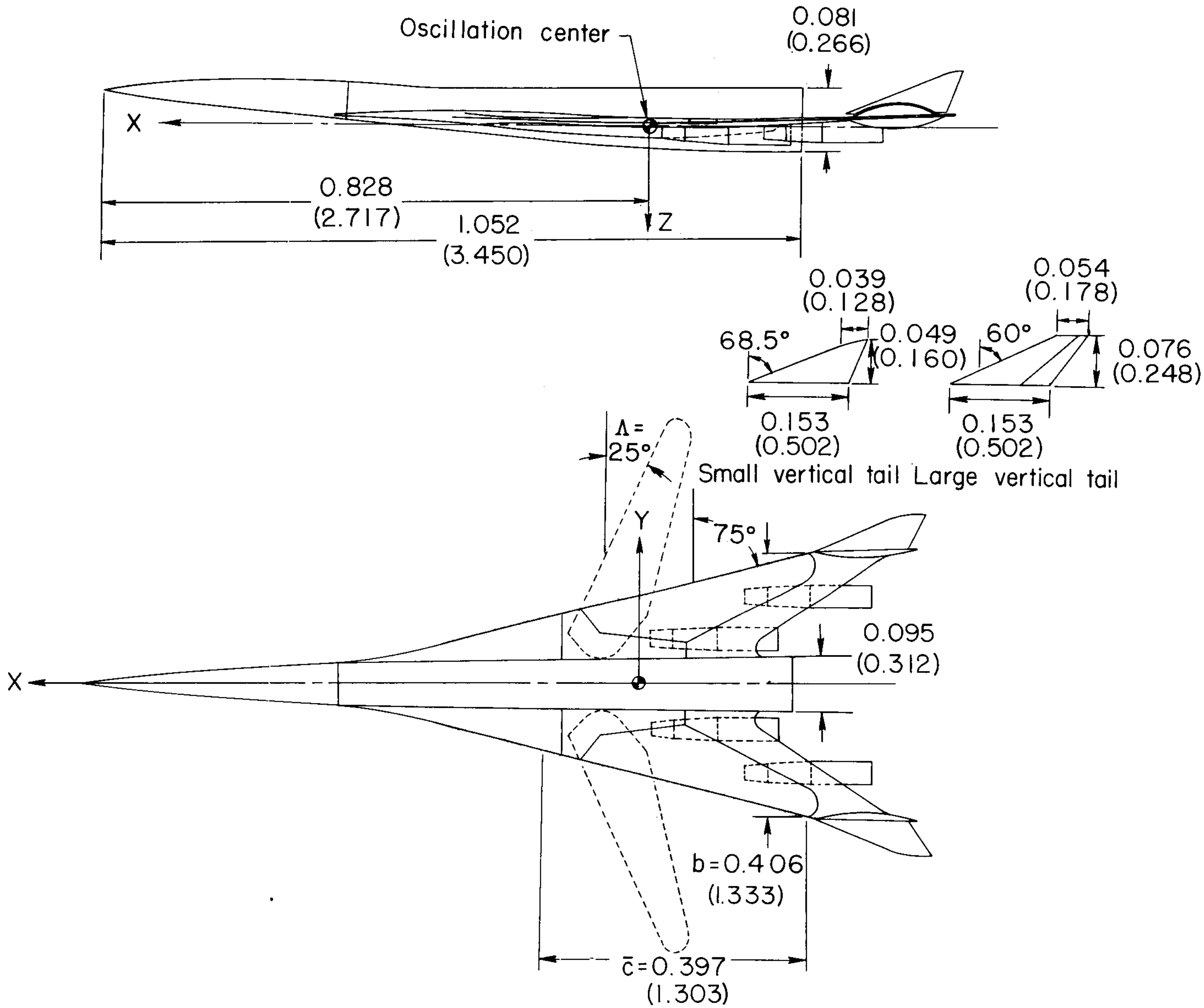

Figure 1.- Sketch of test model. Linear dimensions given first in meters and parenthetically in feet.

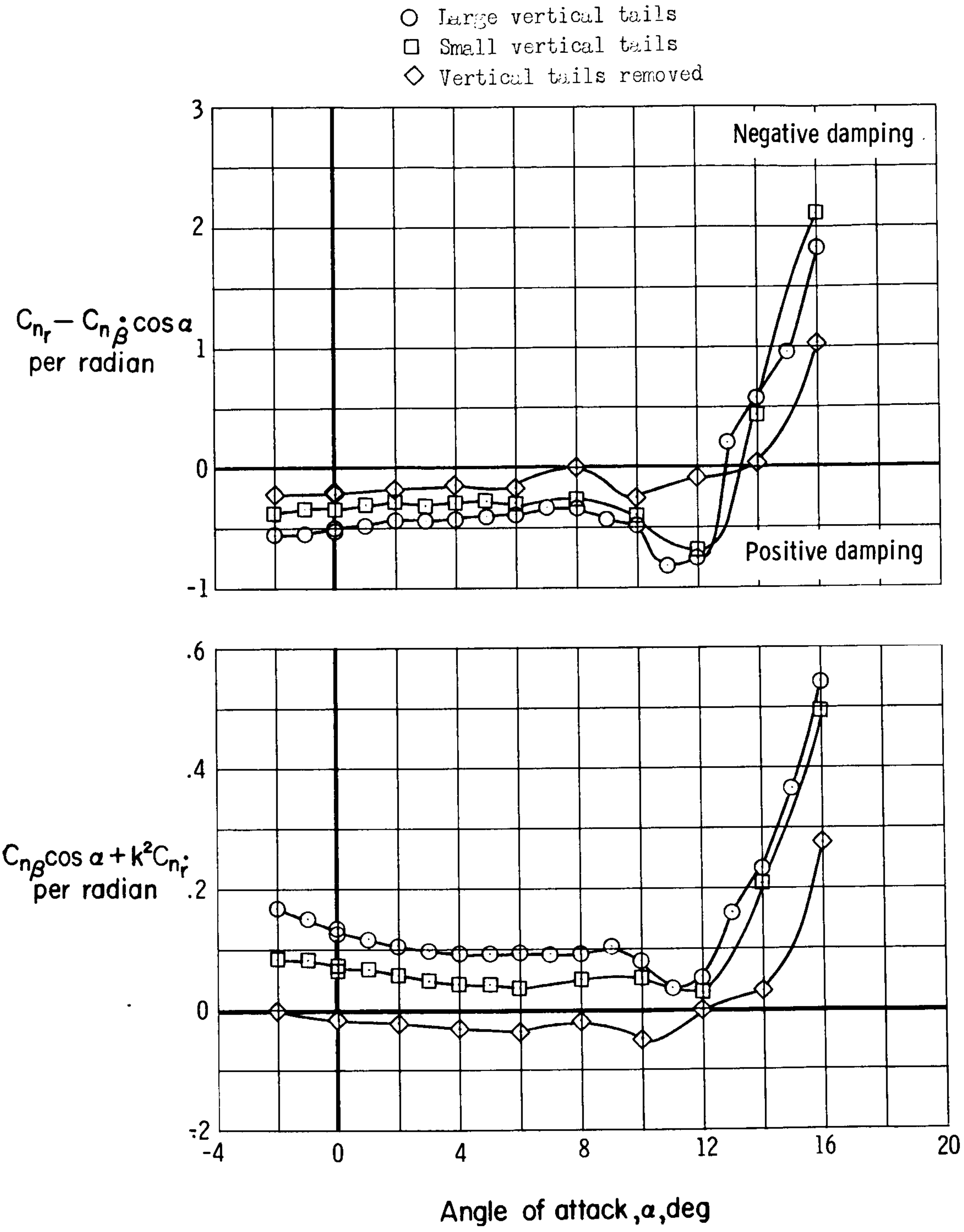

(a) $M = 0.40$; $R = 3.1 \times 10^6$; $k = 0.0432$ to 0.0626.

Figure 2.- Effect of vertical tails on dynamic-stability characteristics in yaw for model with engine inlets open. $\Lambda = 25^0$.

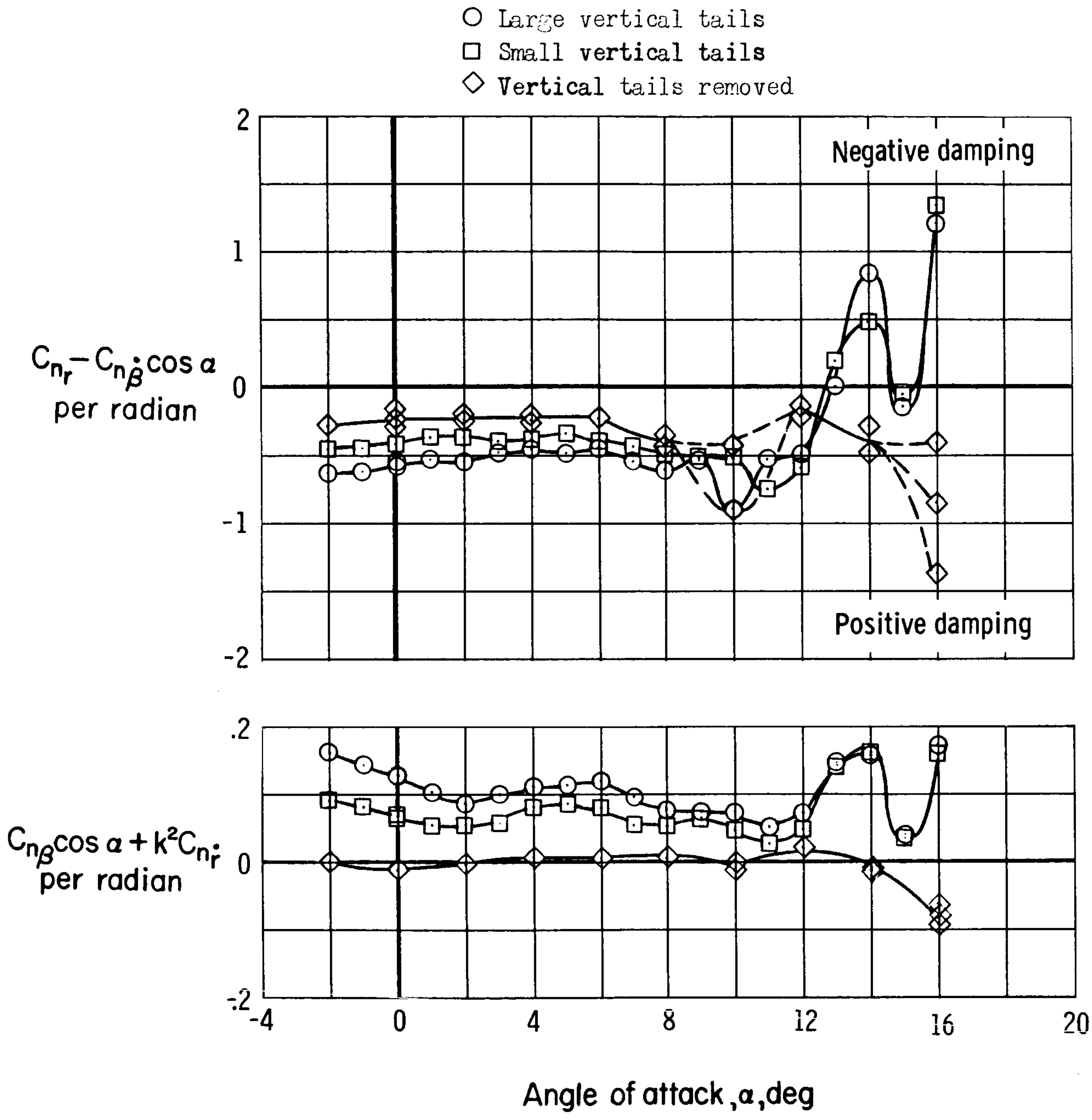

(b) $M = 0.80$; $R = 5.0 \times 10^6$; $k = 0.0175$ to 0.0319.

Figure 2.- Concluded.

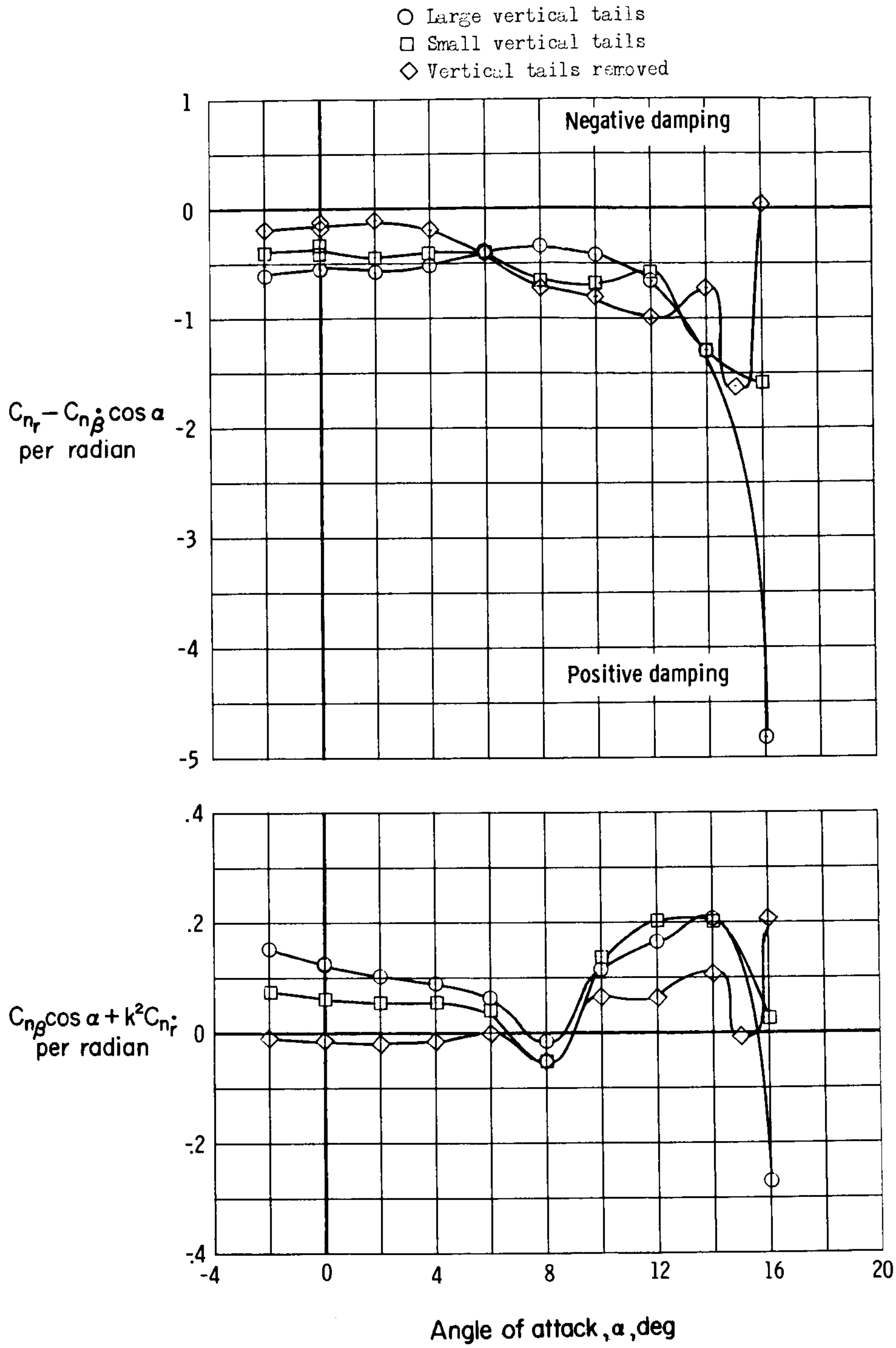

(a) $M = 0.95$; $R = 5.5 \times 10^6$; $k = 0.0163$ to 0.0310.

Figure 3.- Effect of vertical tails on dynamic-stability characteristics in yaw for model with engine inlets open. $\Lambda = 75^{\circ}$.

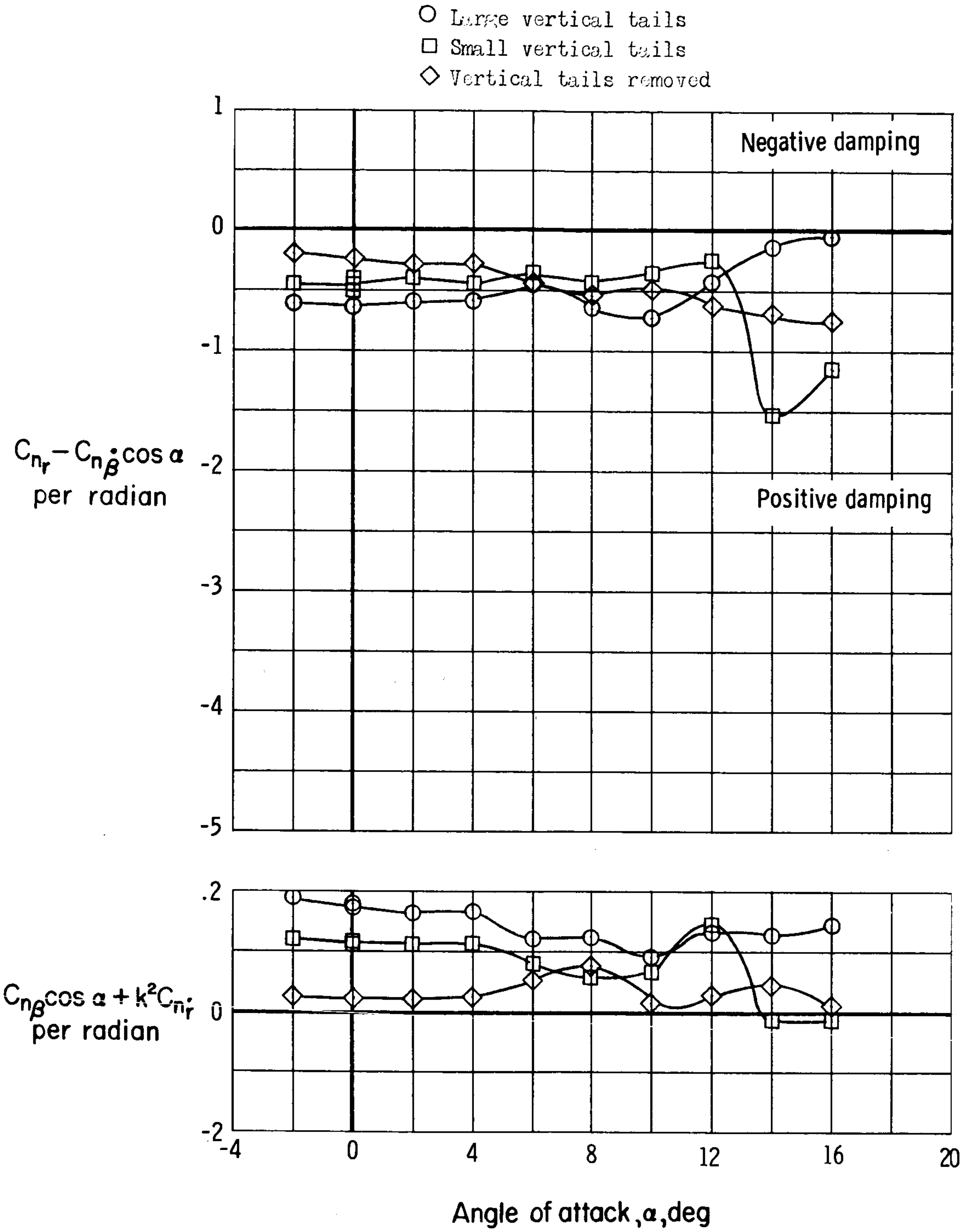

(b) $M = 1.20$; $R = 5.6 \times 10^6$; $k = 0.0154$ to 0.0260.

Figure 3.- Concluded.

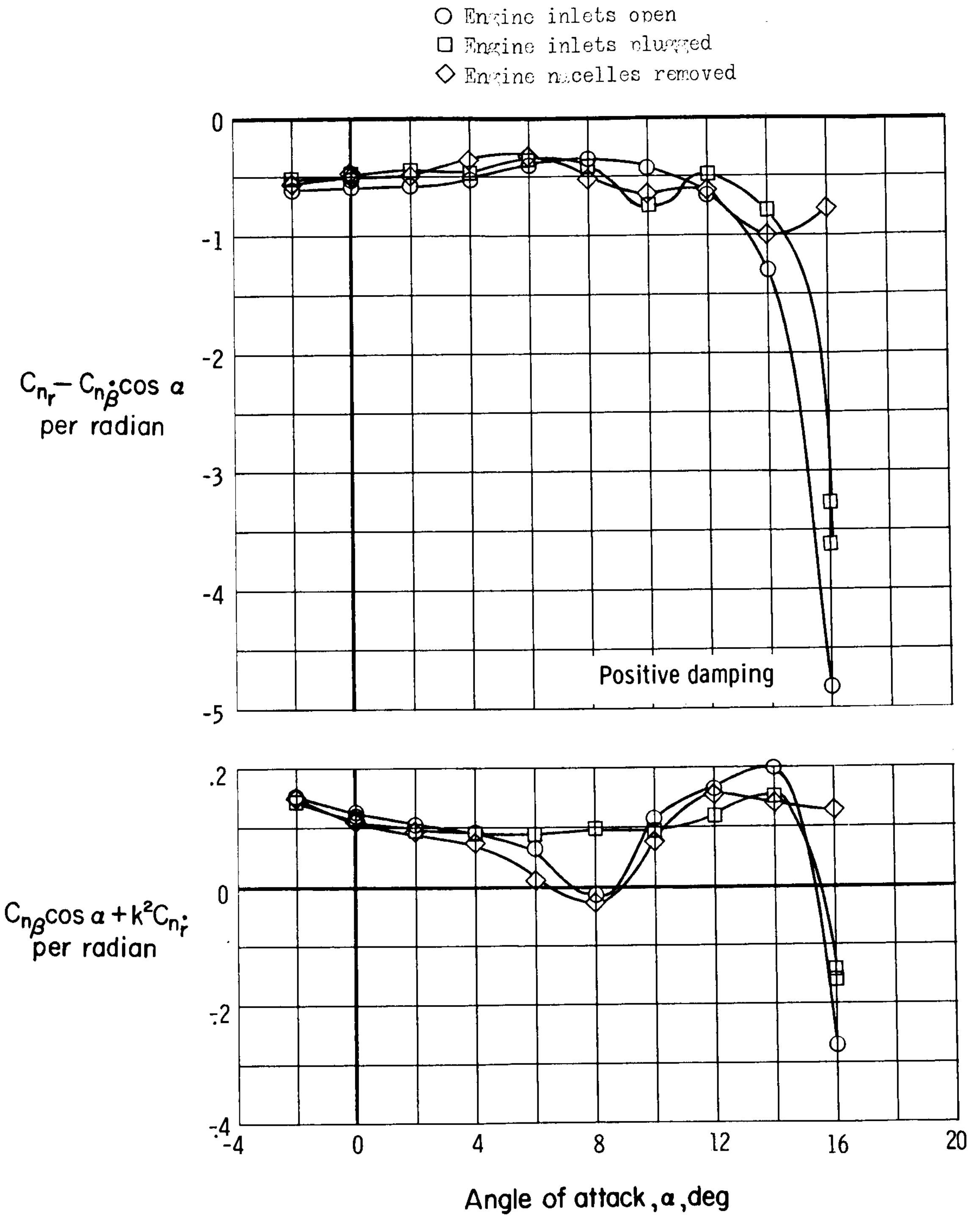

(a) M = 0.95; R = 5.5 × 10^6; k = 0.0193 to 0.0310.

Figure 4.- Effect of engine inlets on dynamic-stability characteristics in yaw for model with large vertical tails. Λ = 75°.

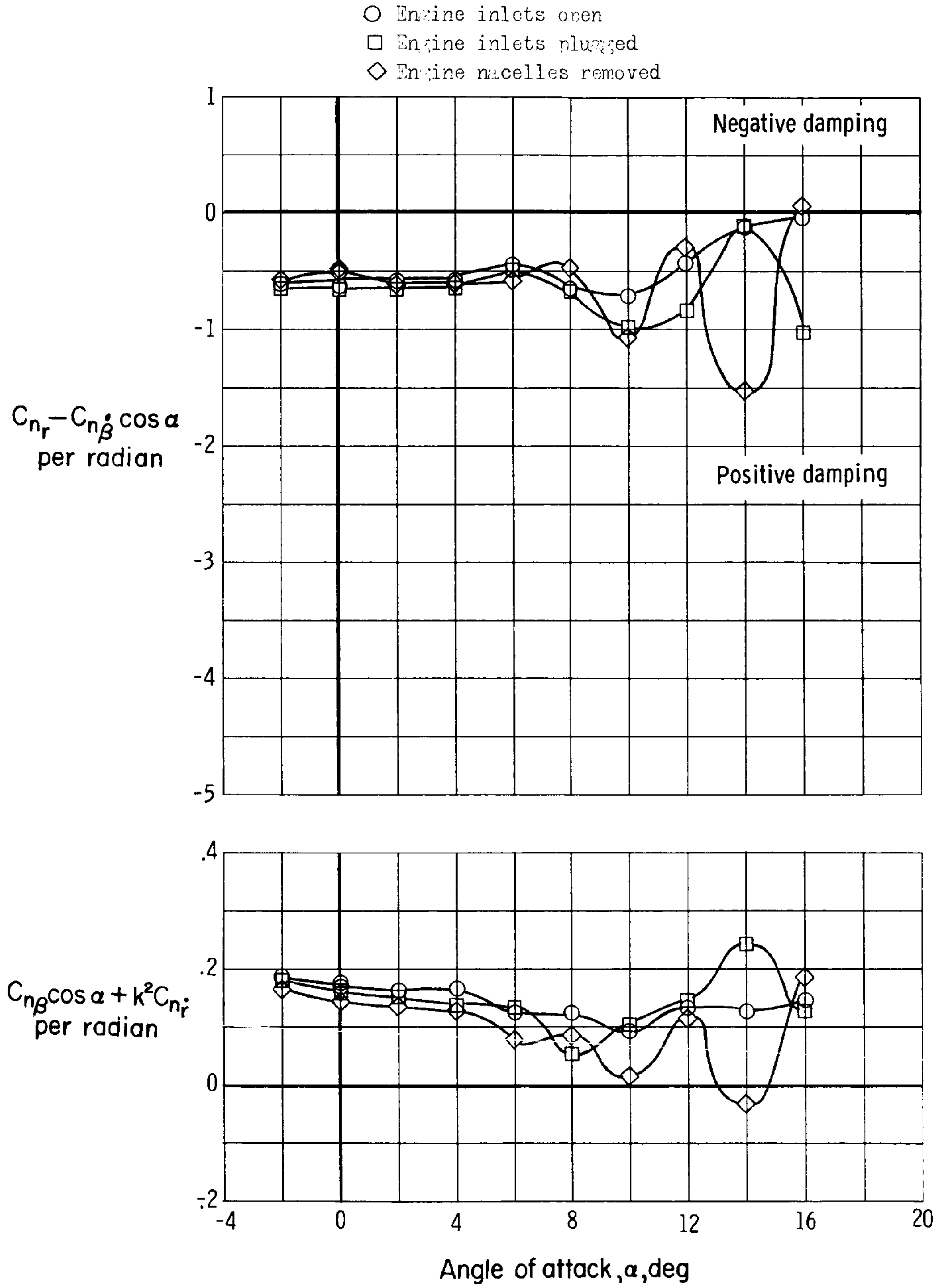

(b) M = 1.20; R = 5.6 × 10^6; k = 0.0152 to 0.0280.

Figure 4.- Concluded.

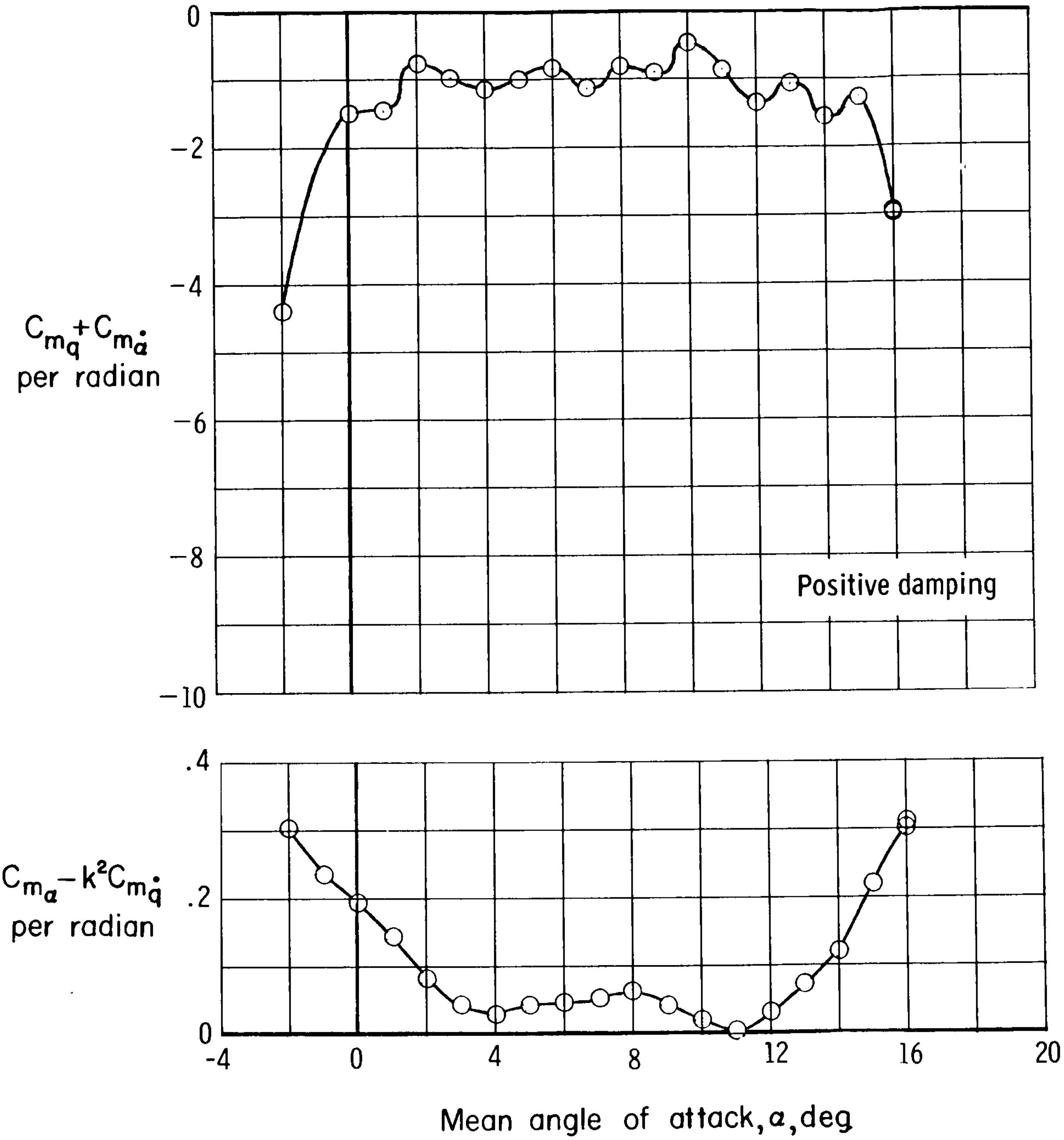

Figure 5.- Dynamic-stability characteristics in pitch for model with large vertical tails and engine inlets open. $\Lambda = 25^{\circ}$; $M = 0.80$; $R = 5.0 \times 10^{6}$; $k = 0.0145$ to 0.0237.

NASA-Langley, 1966 L-4748

"The aeronautical and space activities of the United States shall be conducted so as to contribute . . . to the expansion of human knowledge of phenomena in the atmosphere and space. The Administration shall provide for the widest practicable and appropriate dissemination of information concerning its activities and the results thereof."

—National Aeronautics and Space Act of 1958

NASA SCIENTIFIC AND TECHNICAL PUBLICATIONS

TECHNICAL REPORTS: Scientific and technical information considered important, complete, and a lasting contribution to existing knowledge.

TECHNICAL NOTES: Information less broad in scope but nevertheless of importance as a contribution to existing knowledge.

TECHNICAL MEMORANDUMS: Information receiving limited distribution because of preliminary data, security classification, or other reasons.

CONTRACTOR REPORTS: Technical information generated in connection with a NASA contract or grant and released under NASA auspices.

TECHNICAL TRANSLATIONS: Information published in a foreign language considered to merit NASA distribution in English.

TECHNICAL REPRINTS: Information derived from NASA activities and initially published in the form of journal articles.

SPECIAL PUBLICATIONS: Information derived from or of value to NASA activities but not necessarily reporting the results of individual NASA-programmed scientific efforts. Publications include conference proceedings, monographs, data compilations, handbooks, sourcebooks, and special bibliographies.

Details on the availability of these publications may be obtained from:

SCIENTIFIC AND TECHNICAL INFORMATION DIVISION

NATIONAL AERONAUTICS AND SPACE ADMINISTRATION

Washington, D.C. 20546